Role of Toll-like receptor 4 in intravascular hemolysis-mediated injury

C Vázquez-Carballo *et al. J Pathol* https://doi.org/10.1002/path.5995

Supplementary materials and methods

Supplementary Figures S1–S10

Supplementary materials and methods

RNA extraction and RT-qPCR.

Total RNA from tissues or cultured cells was isolated by the TRIzol method with TRIdity G (Cat# A4051, Panreac, Barcelona, Spain) and reverse-transcribed to cDNA using a High-Capacity cDNA Reverse Transcription Kit (Cat# 4368813, ThermoFisher, Waltham, MA, United States). Expression of target genes was analyzed by RT-qPCR on a ABI Prism 7500 PCR system (Applied Biosystems, Foster City, CA, USA) using Taqman® gene expression assays for mouse *Havcr1* (Mm00506686_m1), *Lcn2* (Mm01324470_m1), *Tlr4* (Mm00445273_m1), *Icam1* (Mm00516023_m1), *Vcam1* (Mm01320970_m1), *Il6* (Mm004 46190_m1), *Ccl2* (Mm00441242_ m1), *Tnf* (Mm00443258_m1), *Hmox1* (Mm00516005_m1), *Fth1* (Mm03030144_g1), *Nfe2l2* (Mm 00477784_m1), *Cat* (Mm00437992_m1) and *Sod1* (Mm01344232_g1). Target gene expression levels were normalized to eukaryotic 18S ribosomal RNA (VIC;Cat# 4310893E, ThermoFisher) and calculated using the $2^{-\Delta\Delta Ct}$ method.

Western blotting

Proteins from tissues or cultured cells were isolated in lysis buffer (50 mM Tris-HCl, 150 mM NaCl, 2 mM EDTA, 2 mM EGTA, 0.2% Triton X-100, 0.3% Igepal) complemented with protease inhibitor cocktail (Cat# P8340, Sigma-Aldrich, St. Louis, MO; USA) and phosphatase inhibitor cocktail (Cat# P0044, Sigma-Aldrich). The samples were then centrifuged for 15 min at 12.000 x *g*, 4 °C. The supernatant was collected, and protein concentration was determined using a BCA protein assay kit (Cat# 23225, ThermoFisher). Proteins (30 µg) from tissue or cultured cell lysates were resolved by SDS-PAGE and transferred to PVDF membranes (Cat# 88518, ThermoFisher). Membranes were blocked with 5% w/v skimmed milk powder in Tris-buffered saline (TBS) with 0.5% v/v Tween-20 (Cat# 10491081, ThermoFisher) for 1 h at room

temperature and incubated with anti phospho-p65 (1:500; Cat# sc-136548, Santa Cruz, Heidelberg, Germany, RRID:AB_10610391), anti phospho-ERK 1/2 (1:1000; Cat# 9101, Cell Signaling, MA, USA, RRID:AB_331646) anti-cleaved PARP1 (1:1000; Cat# ab32064, Abcam, Cambridge, UK, RRID:AB_777102), anti-cleaved caspase 3 (1:1000; Cat# 9661, Cell Signaling, RRID:AB_2341188), anti-HO-1 (1:1000; Cat# ADI-OSA-150-D, Enzo Life Sciences, Farmingdale, NY, USA, RRID:AB_2039235), anti-ferritin (1:1000; Cat# ab86247, Abcam, RRID:AB_1924987), anti-GADPH (1:5000; Cat# MAB374, Sigma-Aldrich, RRID:AB_2107445), and anti-α-tubulin (1:5000; Cat# T6199, Sigma-Aldrich, RRID:AB_477583) overnight at 4 °C. After incubation, membranes were washed with TBS/0.5% Tween-20 and then incubated with corresponding horseradish peroxidase-conjugated donkey anti-rabbit IgG (1:5000; Cat# NA934, GE Healthcare, Erlangen, Germany, RRID:AB_772206) or sheep anti-mouse IgG (1:5000; Cat# NA931, GE Healthcare, RRID:AB_772210) for 1 h at room temperature. After washing with TBS/0.5% Tween-20, blots were developed using an enhanced chemiluminescence method (ECL Luminata Crescendo; Cat# WBLUR0500, Millipore, Burlington, MA, USA). Densitometry analysis was performed using Quantity One 1-D Analysis Software (RRID:SCR_014280) and quantification was expressed in arbitrary densitometric units (AU).

Flow cytometry

In order to assess the expression of TLR4 and TLR2 on the surface of MCT cells by flow cytometry, cultured cells were dissociated with a 0.25% trypsin-EDTA solution (Cat# T4049, Sigma-Aldrich), harvested by centrifugation (5 min, 1200 x *g*, 4 °C) and washed twice with PBS. Cells were labelled for 30 min at 4 °C in the dark with anti-TLR4 PE-conjugated antibody (1:100; Cat# FAB2759P, R&D Systems, Minneapolis, MN, USA, RRID:AB_2044730) or anti-TLR2 APC-conjugated antibody (1:100; Cat# 121810, Biolegend, San Diego, CA, USA, RRID:AB_604151). After incubation, cells were washed with PBS, harvested by centrifugation (5 min, 1200 x *g*, 4 °C), resuspended again in PBS and analyzed with a BD FacsCanto II cytometer (BD Biosciences, San Jose, CA, USA).

Histology, immunohistochemistry and immunofluorescence.

Histological and immunohistochemistry studies were performed in formalin-fixed paraffin-embedded 3 µm tissue sections mounted on Superfrost/Plus microscope slides (Cat# 10149870, ThermoFisher). Signs of histological injury or "non-heme" iron were examined with hematoxylin/eosin in stained tissue sections (Cat# 10034813 and Cat# 6766007,

ThermoFisher). Additionally, renal injury was evaluated following periodic acid-Schiff (PAS) staining (Cat# 3952016, Sigma-Aldrich). Perls's method was used to evaluate the presence of "non-heme" iron in tissues.

F4/80 immunohistochemistry was performed on tissue sections that were deparaffinized then antigen-retrieved using citrate buffer, pH 6.0 (Cat# S1699, Agilent-Dako, Glostrup, Denmark) and the PT link antigen retrieval system (Agilent-Dako). After endogenous peroxidase inactivation with 3% v/v H_2O_2, non-specific antibody binding was blocked in PBS buffer with 4% w/v bovine serum albumin (BSA) (Cat# 10326640, ThermoFisher) and 10% v/v rabbit serum (Cat# C12SA, Bio-Rad, Hercules, CA, USA) for 1 h at room temperature. Then, sections were incubated overnight at 4 °C with rat anti-mouse F4/80 (1:50; Cat# MCA497, Bio-Rad, RRID:AB_2098196) as primary antibody. After overnight incubation, sections were washed in PBS and further incubated for 1 h at room temperature with rabbit anti-rat IgG biotinylated secondary antibody (1:200; Cat# 31834, ThermoFisher, RRID:AB_228448) and 30 min at room temperature protected from light with avidin-biotin peroxidase complex (Vectastain ABC kit, Cat# PK-7200, Vector laboratories, Burlingame, CA, USA). Finally, sections were stained with 3,3'-diaminobenzidine (DAB substrate kit, Cat# ab64238, Abcam), counterstained with hematoxylin (Cat# 10034813, ThermoFisher), mounted with DPX non-aqueous mounting medium (Cat# 100579, Sigma-Aldrich) and then covered with coverslips. Images were taken with a Nikon Eclipse E400 microscope (Nikon, Tokyo, Japan) and Nikon ACT-1 software (Nikon). For kidney sections, the number of F4/80 positive cells per field was counted in 10 randomly selected areas per tissue section at 20x objective magnification. For liver sections, F4/80 positive individual cells could not be visually counted due to the characteristics of the positive staining. F4/80 positive area was quantified using ImageJ 1.53 software (RRID:SCR_003070) in 10 random selected areas per tissue section at 20x objective magnification.

For *in vitro* immunofluorescence studies, MCT were fixed in 4% paraformaldehyde and permeabilized in PBS with 0.2% Triton X-100 (Cat# 10254583, ThermoFisher) for 30 min at room temperature. After non-specific antibody binding was blocked in PBS with 4% w/v bovine serum albumin (BSA) (Cat# 10326640, ThermoFisher), fixed cells were incubated with rabbit anti-p65 (1:100; Cat# 8242, Cell Signaling, RRID:AB_10859369) as primary antibody overnight at 4 °C followed by Alexa Fluor 488 conjugated secondary antibody (1:200; Cat# A11090; ThermoFisher, RRID:AB_221562) for 1 h at room temperature. Nuclei were stained with 4'-6-

diamidino-2-phenylindole (DAPI; Cat# D9542, Sigma-Aldrich) and slides were mounted with FluorSave (Cat# 345789, Millipore). Images were taken with a Leica TCS SP5 inverted confocal microscope.

TUNEL assay

The extent of cell death was estimated using a terminal deoxynucleotidyl transferase dUTP nick-end labeling (TUNEL) assay. Detection of DNA fragmentation was performed using an ApopTag® Fluorescein *In Situ* Apoptosis Detection Kit (Cat# S7110, Sigma-Aldrich) following the manufacturer's instruction. Nuclei were stained with 4'-6-diamidino-2-phenylindole (DAPI; Cat# D9542, Sigma-Aldrich) and slides were mounted with FluorSave (Cat# 345789, Millipore). Images were captured using a Leica TCS SP5 inverted confocal microscope. The number of TUNEL-positive cells per field was counted in at least 10 random selected areas per tissue section at 20x objective magnification. The mean number of labeled cells per field was expressed as the number of TUNEL-positive cells.

Heme concentration in tissues

Heme concentration in the kidney, spleen and liver was determined using a commercial assay (Cat# MAK-316, Sigma-Aldrich)

Supplementary Figures S1–S10

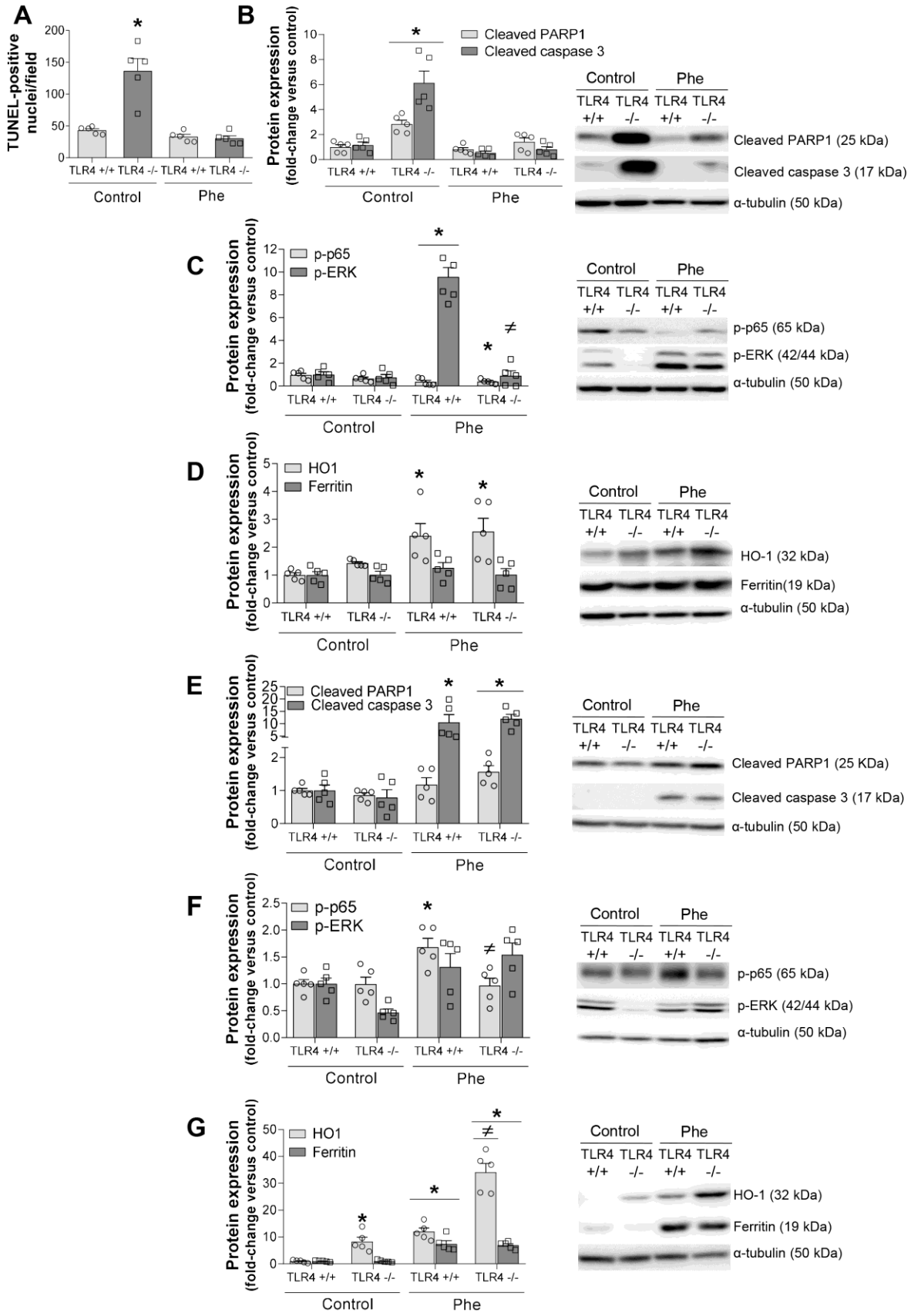

Figure S1. TLR4 deficiency has a limited effect in cell-death and inflammation in spleen and liver after hemolysis. (A) Quantification of TUNEL-positive cells in spleens after intravascular hemolysis in *Tlr4* $^{+/+}$ and *Tlr4* $^{-/-}$ mice. (B) Representative blot images and quantification of cleaved caspase 3 and cleaved PARP1, and (C) p65 NF-κB and ERK1/2 phosphorylation levels and (D) protein levels of heme oxygenase 1 (HO-1) and Ferritin in spleen assessed by western blotting. (E) Representative images and quantification of protein levels in the liver of cleaved caspase 3 and PARP1, and (F) phosphorylated p65 NF-κB and ERK1/2, and (G) HO-1 and Ferritin determined by western blotting. Results are expressed as mean ± SEM (n=5). * $p < 0.05$ versus *Tlr4* $^{+/+}$control mice, ≠ $p < 0.05$ versus *Tlr4* $^{+/+}$ Phe-injected mice.

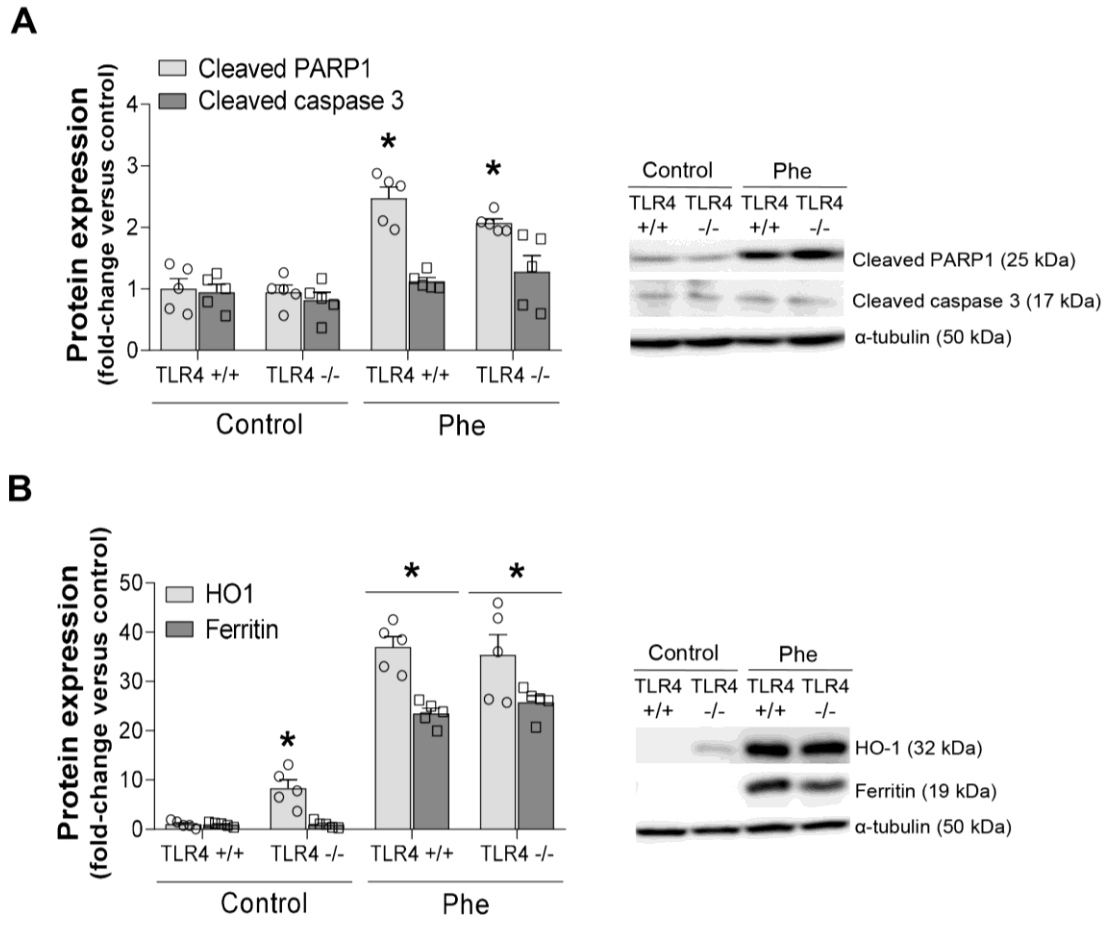

Figure S2. TLR4 deficiency did not protect against hemolysis-mediated apoptosis in kidney after hemolysis. (A) Cleaved caspase 3 and cleaved PARP1 protein expression quantification and representative western blotting images for kidneys after hemolysis induction in *Tlr4* $^{+/+}$ and *Tlr4* $^{-/-}$ mice. (B) Renal protein levels of heme oxygenase 1 (HO1) and Ferritin in kidney assessed by western blotting; quantification and representative images. Results are expressed as mean ± SEM (n=5). * $p < 0.05$ versus *Tlr4* $^{+/+}$ control mice, ≠ $p < 0.05$ versus *Tlr4* $^{+/+}$ Phe-injected mice.

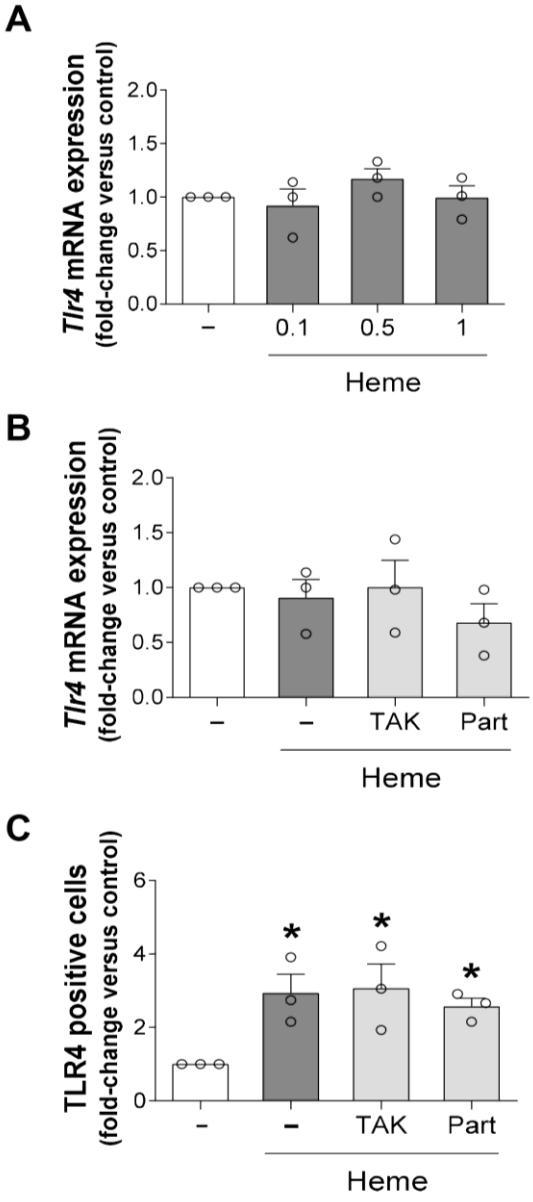

Figure S3. Inhibition of NF-kB and ERK1/2 pathways did not modify heme-mediated TLR4 expression in renal cells. (A) *Tlr4* mRNA levels measured by RT-qPCR in MCTs cells exposed for 6 h to different heme concentrations (0–1 µM). (B) Gene expression of *Tlr4* determined by RT-qPCR after heme stimulation for 6 h. (C) Cell surface TLR4 levels measured by flow cytometry in MCTs cells treated with heme for 24 h. MCTs were pretreated with TAK-242 (TAK) for 4 h or parthenolide (Part) for 1 h and then stimulated with heme (1 µM). Results are expressed as mean ± SEM from n=3 independent experiments. * $p < 0.05$ versus non-treated cells, ≠ $p < 0.05$ versus heme-treated cells.

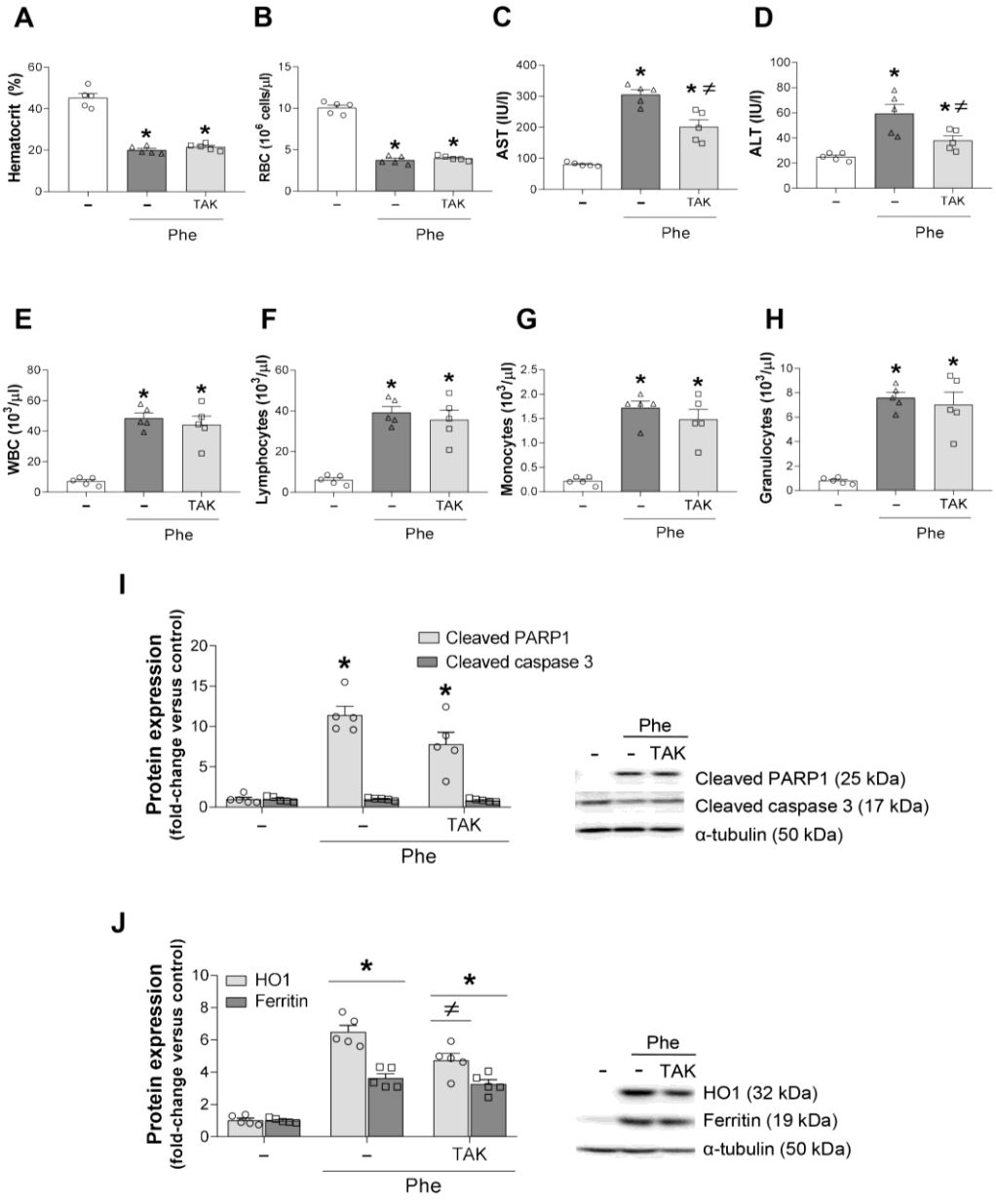

Figure S4. TLR4 pharmacological inhibition did not modify hematological parameters, circulating immune cells or hemolysis-mediated apoptosis of renal cells. (A) Hematocrit and (B) total red blood cells (RBCs) measured in fresh blood in Control and Phe-injected mice with or without TAK-242 administration (1 h before induction of hemolysis). Serum measurements of (C) aspartate transaminase (AST) and (D) alanine transaminase (ALT) levels. Circulating populations of (E) white blood cells (WBCs), (F) lymphocytes, (G) monocytes and (H) granulocytes were measured in fresh blood using a hematological cell counter analyzer. (I) Renal expression of cleaved caspase 3 and cleaved PARP1; quantification and representative images as measured by western blotting. (J) Protein levels of heme oxygenase 1 (HO1) and ferritin in kidney assessed by western blotting; quantification and representative images.

Results are expressed as mean ± SEM (n=5). * $p < 0.05$ versus control mice, ≠ $p < 0.05$ versus Phe-injected mice.

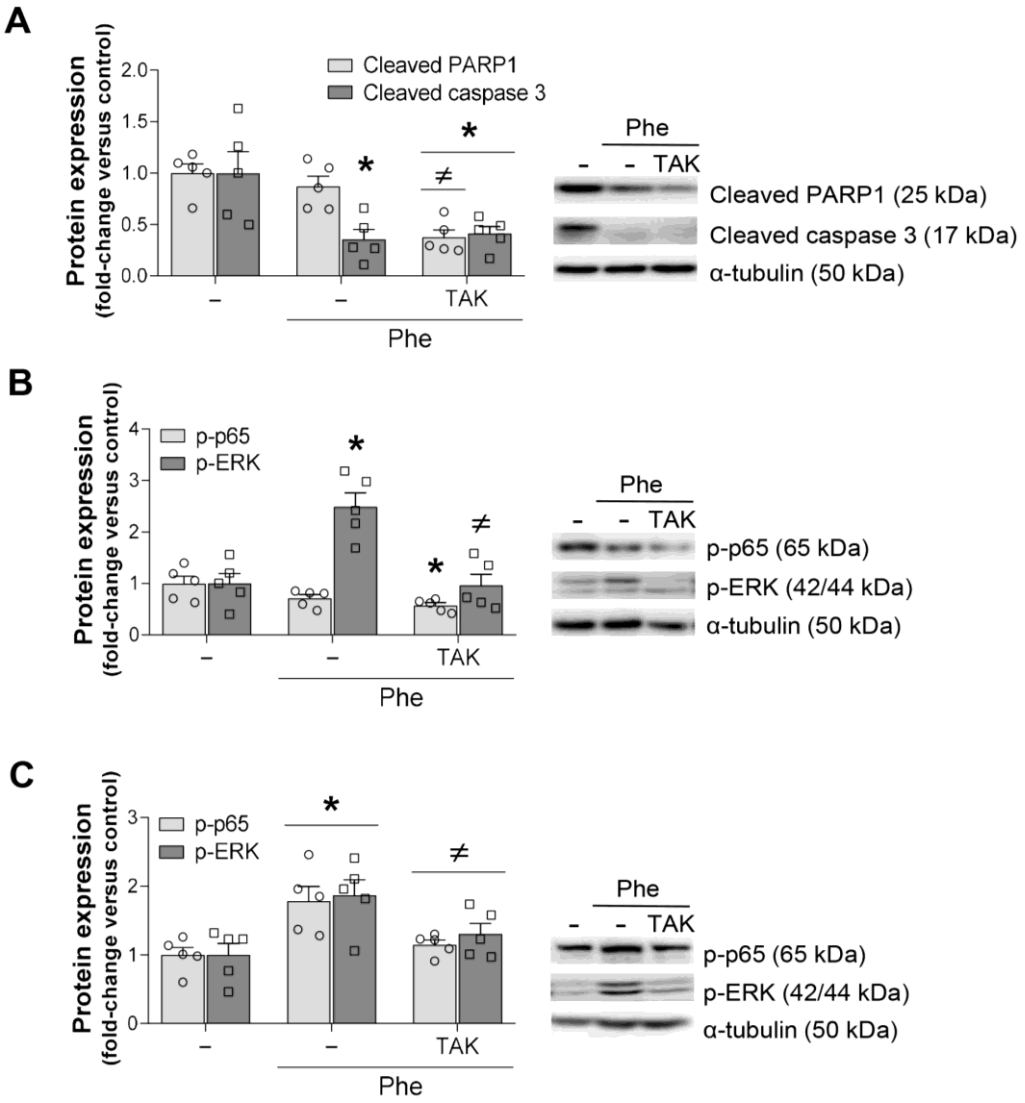

Figure S5. Apoptosis and inflammatory pathways in spleen and liver after TLR4 inhibition in mice with hemolysis. (A) Splenic expression of cleaved caspase 3 and PARP1 quantification and representative images measured by western blotting in control and Phe-injected mice with or without TAK242 administration (1 h before induction of hemolysis). Representative images and quantification of protein levels of phosphorylated p65 NFkB and ERK1/2 determined by western blotting in (B) spleen and (C) liver. Results are expressed as mean ± SEM (n=5). * $p < 0.05$ versus control mice, ≠ $p < 0.05$ versus Phe-injected mice.

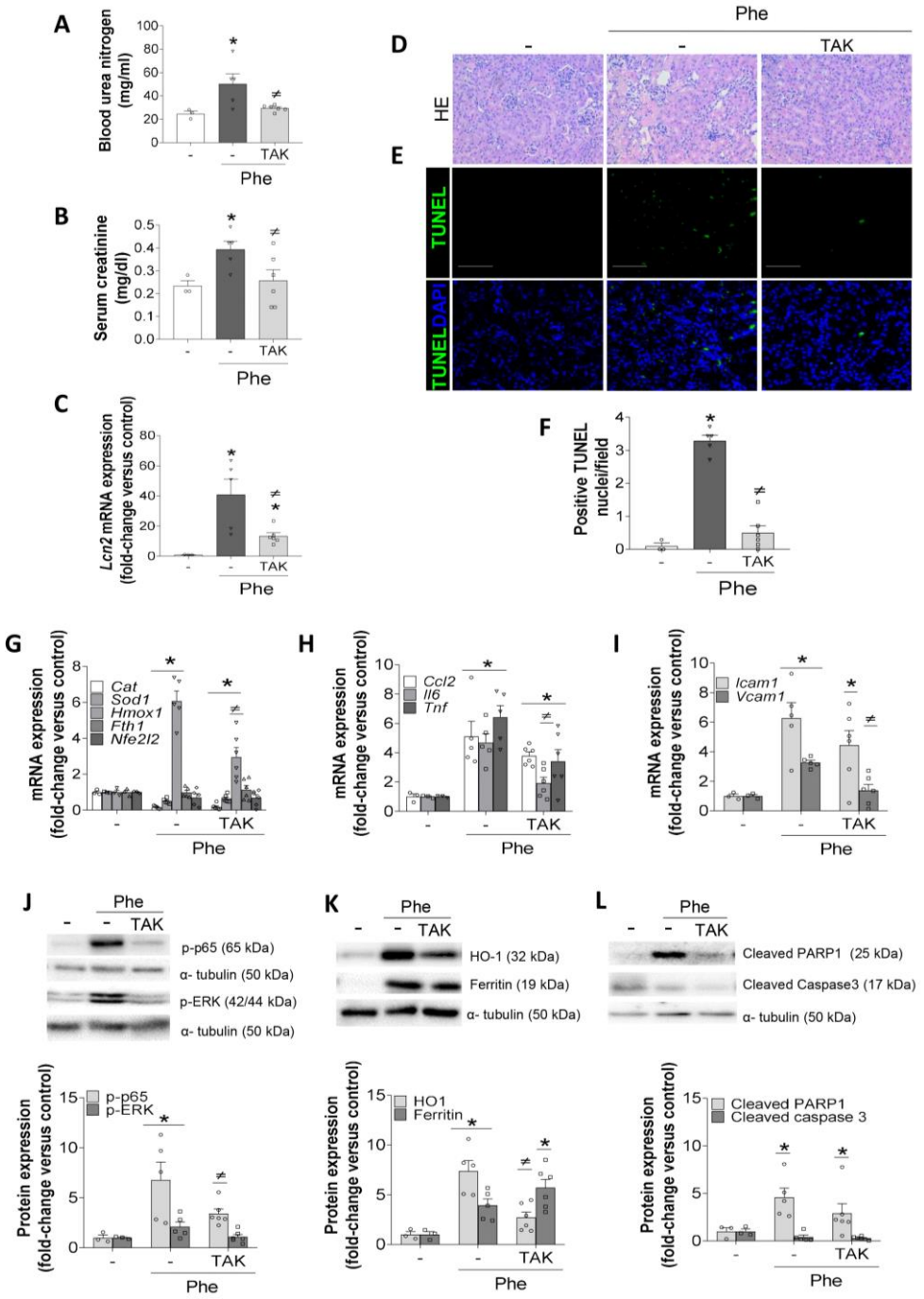

Figure S6. TLR4 pharmacological inhibition reduces renal injury associated to hemolysis. Serum levels of (A) blood urea nitrogen (BUN) and (B) creatinine in control and Phe-injected mice with or without TAK-242 administration (4 h before induction of hemolysis). (C) Expression of tubular injury marker Ngal (*Lcn2*) as determined by RT-qPCR. (D) Representative images showing hematoxylin/eosin staining of paraffin embedded renal sections at 20X objective magnification. (E) Representative images and (F) quantification of TUNEL-positive cells (green) in renal sections. Nuclei were stained with DAPI (blue). Scale bar, 200 µm. Renal gene expression of (D) catalase (*Cat*), superoxide dismutase (*Sod1*), heme oxygenase 1 (*Hmox1*), ferritin (*Fth1*) and Nrf2 (*Nfe2l2*) and (E) *Ccl2, Il6* and *Tnf* and (F) *Icam1* and *Vcam1* as determined by RT-qPCR. (G) Western blot quantification and representative images showing phosphorylation levels of p65 NF-κB and ERK1/2, (H) cleaved PARP1 and caspase 3, (I) HO-1 and Ferritin. Results are expressed as mean ± SEM (n=5). * $p < 0.05$ versus control mice, ≠ $p < 0.05$ versus Phe-injected mice.

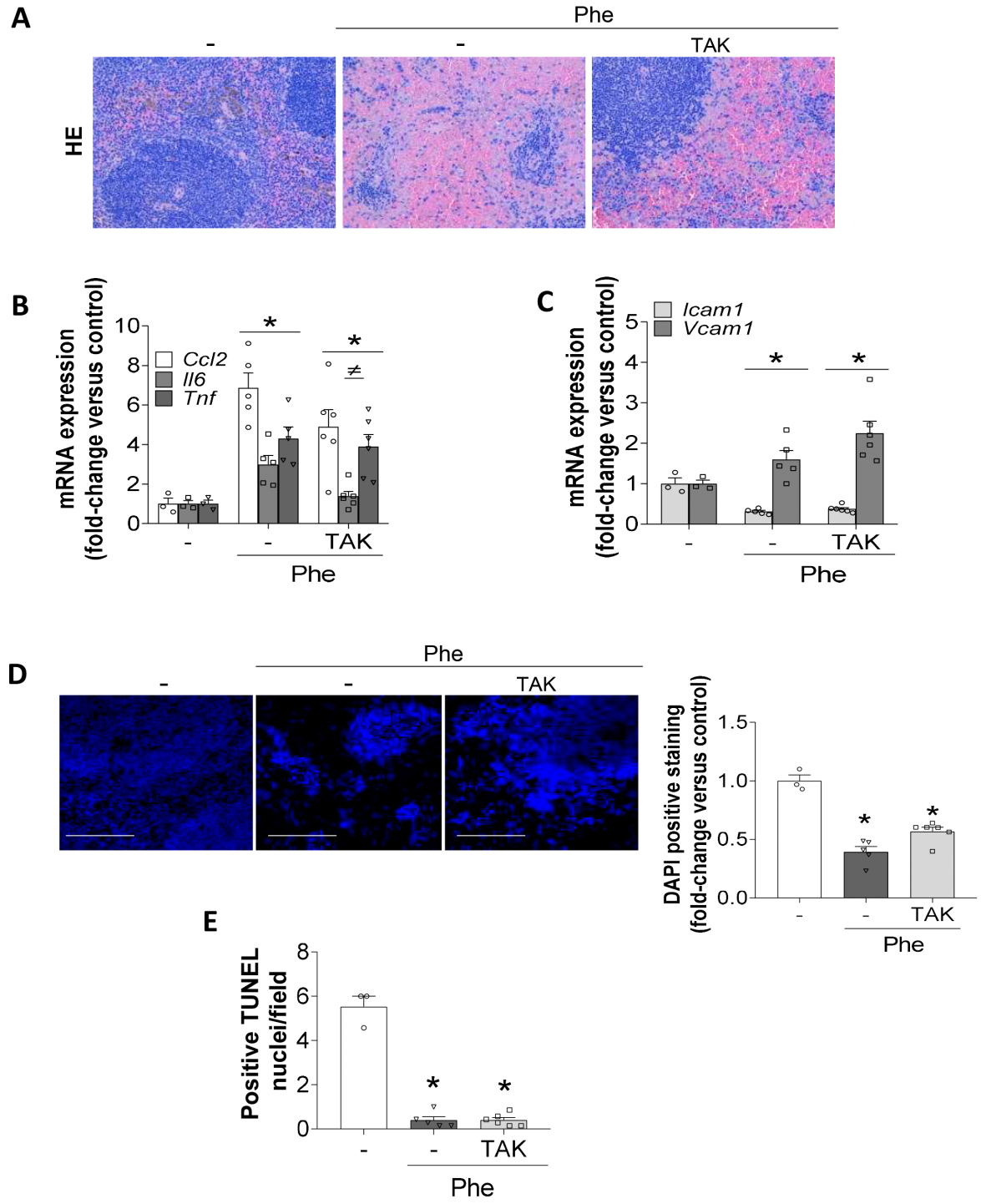

Figure S7. Effects of TLR4 pharmacological inhibition in spleen after induction of hemolysis. (A) Representative images showing hematoxylin/eosin staining of paraffin embedded spleen sections of control and Phe-injected mice with or without TAK-242 administration (4 h before induction of hemolysis), at 20X objective magnification. Gene expression of (B) *Ccl2, Il6* and *Tnf* and (C) *Icam1* and *Vcam1* as determined by RT-qPCR. (D) Representative confocal microscopy images and quantification of splenic DAPI-positive cells (blue). Scale bar, 100 µm. (E) Quantification of TUNEL-positive cells in spleen sections. Results are expressed as mean ± SEM (n=5). * $p < 0.05$ versus control mice, ≠ $p < 0.05$ versus Phe-injected mice.

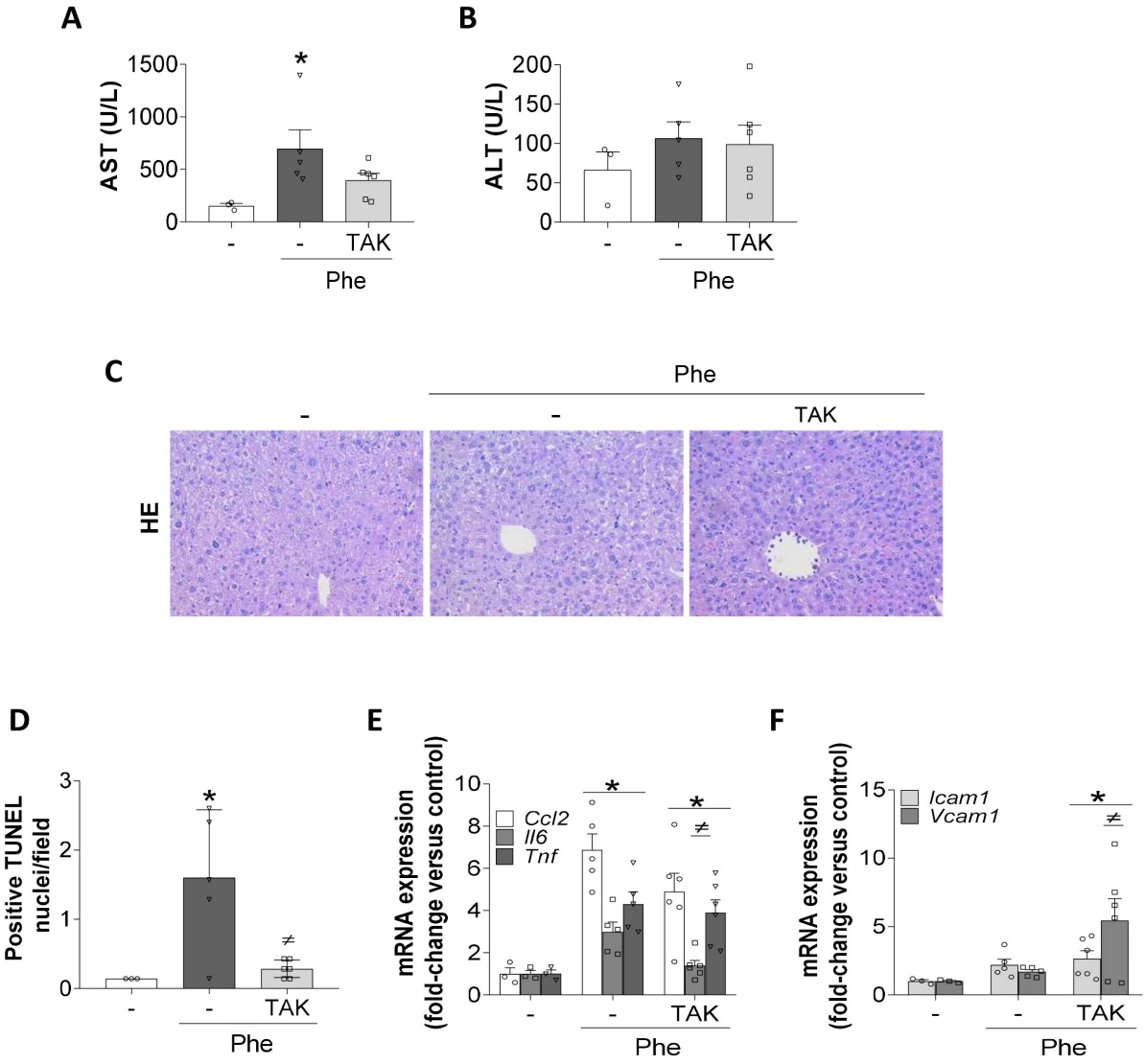

Figure S8. Effects of TLR4 pharmacological inhibition in liver after induction of hemolysis. Serum levels of (A) aspartate transaminase (AST) and (B) alanine transaminase (ALT) in control and Phe-injected mice with or without TAK-242 administration (4 h before induction of hemolysis). (C) Representative images showing hematoxylin/eosin staining of paraffin embedded liver section at 20X objective magnification. (D) Quantification of TUNEL positive cells in liver sections. Gene expression of (E) *Ccl2, Il6* and *Tnf*, and (F) *Icam1* and *Vcam1* as determined by RT-qPCR. Results are expressed as mean ± SEM (n=5). * $p < 0.05$ versus control mice, ≠ $p < 0.05$ versus Phe-injected mice.

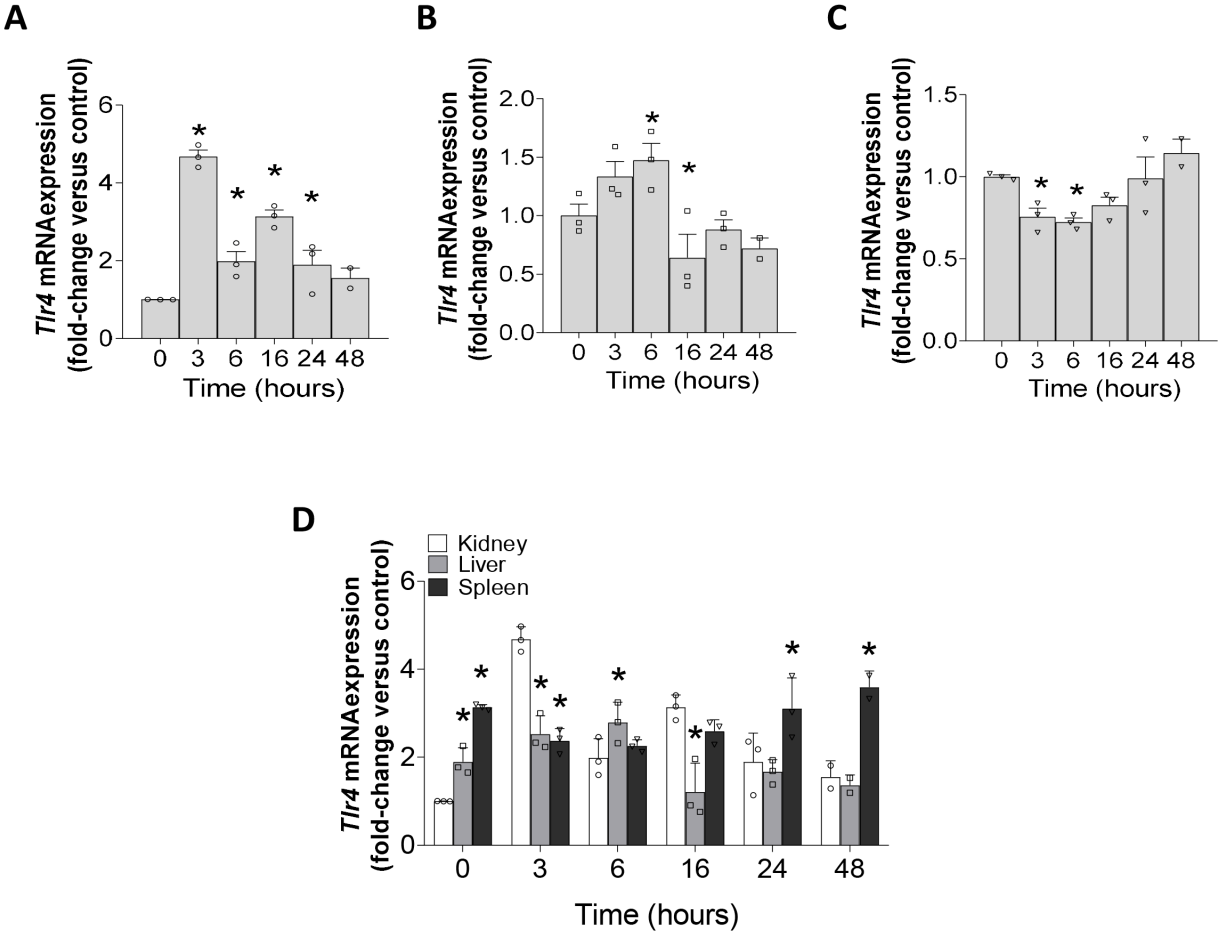

Figure S9. *Tlr4* gene expression in tissues after induction of hemolysis. *Tlr4* gene expression in (A) kidney, (B) liver, and (C) spleen determined by RT-qPCR after induction of intravascular hemolysis (Phe 200 mg/kg). * $p < 0.05$ versus control. (D) Global *Tlr4* expression in kidney, liver and spleen determined by RT-qPCR. Results are expressed as mean ± SEM (n=3). * $p < 0.05$ versus kidney at each specific time point.

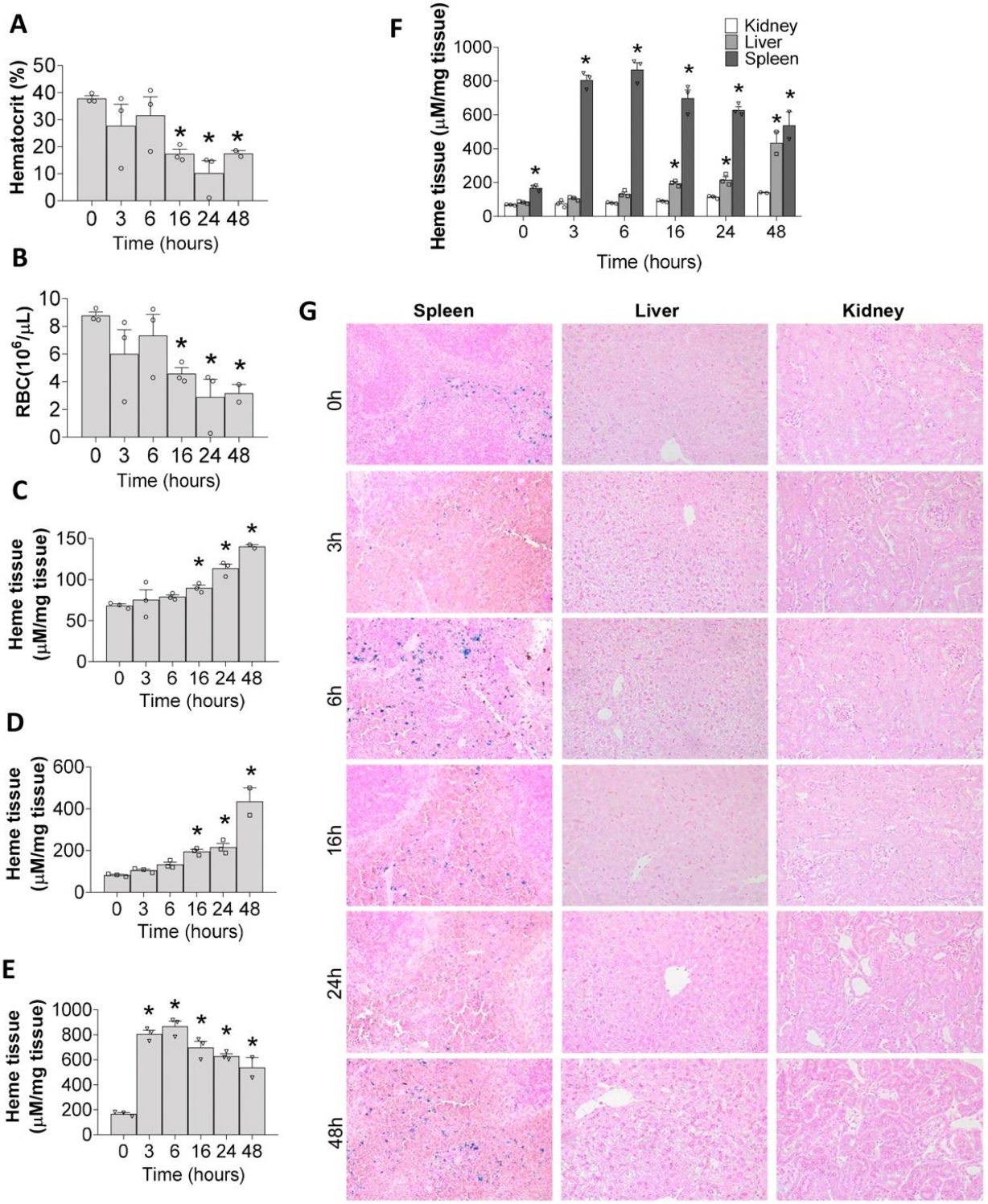

Figure S10. Hematological parameters and heme content in tissues after induction of hemolysis. (A) Serum measurement of blood urea nitrogen (BUN) and (B) creatinine in mice with intravascular hemolysis (Phe 200 mg/kg). Heme concentration in (C) kidney, (D) liver and (E) spleen. * $p < 0.05$ versus control. (F) Global representation of heme concentration in kidney, liver, and spleen. (G) Representative images of blue Pearls' staining at 0, 3, 6, 16, 24 and 48 h after induction of hemolysis in kidney, liver, and spleen sections at 20X objective magnification. Results are expressed as mean ± SEM (n=3). *. $p < 0.05$ versus kidney at each specific time point.